

## Investigation of anomalously high transition strength for the $2_1^+$ state in $^{174}\text{Os}$ through lifetime measurement

C. B. Li,<sup>1,2</sup> X. G. Wu,<sup>1,\*</sup> X. F. Li,<sup>2,†</sup> C. Y. He,<sup>1</sup> Y. Zheng,<sup>1</sup> G. S. Li,<sup>1</sup> S. H. Yao,<sup>1</sup> S. P. Hu,<sup>1,3</sup> H. W. Li,<sup>1,2</sup> J. L. Wang,<sup>1</sup> J. J. Liu,<sup>1,3</sup> C. Xu,<sup>4</sup> J. J. Sun,<sup>4</sup> and W. W. Qu<sup>5</sup>

<sup>1</sup>China Institute of Atomic Energy, Beijing 102413, China

<sup>2</sup>College of Physics, Jilin University, Changchun 130012, China

<sup>3</sup>College of Physics and Technology, Shenzhen University, Shenzhen 518060, China

<sup>4</sup>School of Physics and State Key Laboratory of Nuclear Physics and Technology, Peking University, Beijing 100871, China

<sup>5</sup>School of Physics and Nuclear Energy Engineering, Beihang University, Beijing 100191, China

(Received 19 June 2012; published 19 November 2012)

The lifetime of the  $2_1^+$  state in  $^{174}\text{Os}$  was measured in a fast timing experiment using  $\text{LaBr}_3(\text{Ce})$  crystals for  $\gamma$ -ray detection. The excellent energy resolution in conjunction with the superb time properties of the new material allows for the reliable handling of the background, thus providing very precise lifetime values. The resulting  $B(E2, 2_1^+ \rightarrow 0_1^+)$  transition strength is discussed in relation to the systematics of the previously reported  $B(E2, 2_1^+ \rightarrow 0_1^+)$  values in the Os isotopes and compared to predictions of several models. The maximum of the transition probabilities of the  $2_1^+$  states at  $N = 98$  for W and Os nuclei may be interpreted as resulting from the effects of the deformed subshell at  $N = 98$  as well as the “intruder” proton  $h_{9/2}$  orbital.

DOI: [10.1103/PhysRevC.86.057303](https://doi.org/10.1103/PhysRevC.86.057303)

PACS number(s): 21.10.Tg, 23.20.-g, 27.70.+q

Measurements of excitation transition probabilities are useful for studying nuclear structure. Reduced transition probabilities of first  $2^+$  states,  $B(E2, 2_1^+ \rightarrow 0_1^+)$ , for even-even nuclei are important in evaluating nuclear collectivity. Among these measurements, nuclei in the transitional region of isotopes having a mass number of around 170 still attract attention because they provide an opportunity to study the transition from spherical structures to deformed axially symmetric rotors. From the standpoint of the  $R_{4/2} \equiv E(4_1^+)/E(2_1^+)$  ratio,  $^{174}\text{Os}$  with a value of 2.74, which is below the value of 2.90 predicted by the  $X(5)$  [1] solution and certainly lower than the value of 3.33 for the rigid rotor limit, appears to lie slightly in the vibrational region, as shown in Fig. 1(a). However,  $^{174}\text{Os}$ , which has a maximal  $B(E2, 2_1^+ \rightarrow 0_1^+)$  value [see Fig. 1(b)], points to a more deformed nature from phenomenology and does not seem to follow the trends in the neighboring nuclei [2]. In addition, it is also difficult to account for this finding in any modern theory [3]. But from Fig. 1(b), one can see that the  $B(E2, 2_1^+ \rightarrow 0_1^+)$  of the isotope  $^{174}\text{Os}$  has a relatively large experimental uncertainty. Therefore new measurements with a higher accuracy will be needed for checking whether an interesting structural effect causes this anomaly or whether the error bars were underestimated on the data point.

Lifetimes of  $2_1^+$  states in well-deformed nuclei of the rare-earth region are typically in the range of hundreds of picoseconds to 1 ~ 2 ns. A variety of experimental methods have been developed for their measurements. The recoil distance method (RDM) using the so-called plunger devices, which take advantage of the superb energy resolution of Ge detectors, have been developed to deduce state lifetimes between ~1 ps and ~1 ns. Another method using a mix of

Ge, plastic,  $\text{BaF}_2$ , or  $\text{LaBr}_3(\text{Ce})$  detecting devices employing triple- $\beta\gamma\gamma$  coincidence measurements, designed for use in  $\beta$  decay, measures the lifetimes of nuclear states down to tens of picoseconds and is especially suitable for the investigation of neutron-rich nuclei [4,5]. Very recently, a new experimental method with  $\text{LaBr}_3(\text{Ce})$  detectors in combination with the power of the Ge array, employing triple- $\gamma$  coincidence measurements, has been developed to deduce state lifetimes longer than tens of picoseconds [6,7]. The method is especially suitable for in-beam  $\gamma$ -ray spectroscopy measurements where it was applied in many cases [6–8]. In this new method, triple- $\gamma$  coincidences are measured with an array containing both HPGe and  $\text{LaBr}_3(\text{Ce})$  detectors. The high-energy resolution of the Ge detectors is used to select the desired  $\gamma$ -ray cascade, and the array of fast  $\text{LaBr}_3(\text{Ce})$  to build the delayed coincidence time spectra for selected levels.

In this Brief Report, we report on using this new triple- $\gamma$  coincidences method to remeasure the lifetime of the  $2_1^+$  state in  $^{174}\text{Os}$ . This method applied in a delayed coincidence technique provides a more reliable value compared with earlier measurements with the plunger method [9] because the measured value of ~1 ns is at the limit of the technique, causing a large error in the measurement of this relatively long lifetime.

The excited states in  $^{174}\text{Os}$  were populated using the  $^{150}\text{Sm} (^{28}\text{Si}, 4n) ^{174}\text{Os}$  reaction at a beam energy of 140 MeV. The target consisted of a 0.9 mg/cm<sup>2</sup>  $^{150}\text{Sm}$  rolled onto a 12.5 mg/cm<sup>2</sup> Pb backing. The experiment was performed at the HI-13 tandem accelerator of the China Institute of Atomic Energy. The lifetimes of the states of interest were determined by using a fast timing setup consisting of four  $\text{LaBr}_3(\text{Ce})$  scintillator detectors working in coincidence with 11 Compton-suppressed HPGe detectors. The four  $\text{LaBr}_3(\text{Ce})$  detectors were mounted below the target chamber on a ring of approximately 90° with respect to the beam axis. All four  $\text{LaBr}_3(\text{Ce})$  detectors have crystals with a size of 30 mm in

\*Corresponding author: wxg@ciae.ac.cn

†Corresponding author: lixf@jlu.edu.cn

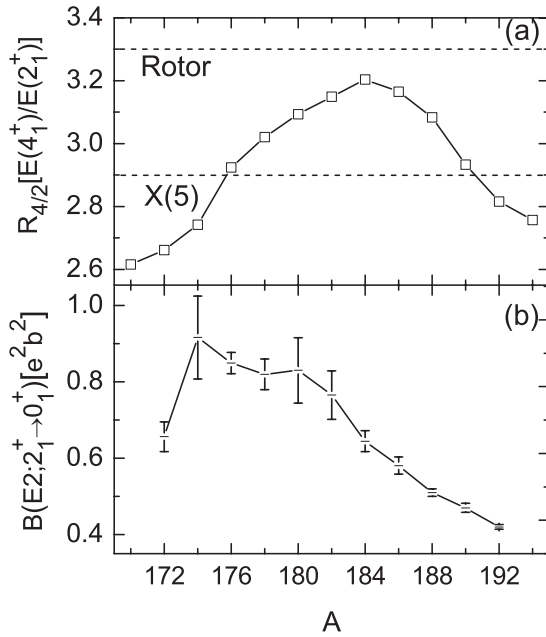


FIG. 1. (a) The ratios of the energies of the  $4_1^+$  and  $2_1^+$  states across the Os isotopic chain. (b) Corresponding  $B(E2, 2_1^+ \rightarrow 0_1^+)$  values are displayed. The  $B(E2, 2_1^+ \rightarrow 0_1^+)$  data are taken from Ref. [10], except for  $^{176}\text{Os}$  [11],  $^{178}\text{Os}$  [12], and  $^{180}\text{Os}$  [3]. Lines are drawn to guide the eye.

height and a diameter of 40 mm and they were coupled to an XP2020Q photomultiplier tube. At first, we performed off-line tests with standard radioactive sources ( $^{22}\text{Na}$ ,  $^{60}\text{Co}$ ,  $^{133}\text{Ba}$ , and  $^{152}\text{Eu}$ ) to optimize the performance of our fast timing setup. For the 1274.5-keV  $\gamma$  ray of  $^{22}\text{Na}$ , the energy resolution was 2.4%, while for the 121.8-keV  $\gamma$  ray of  $^{152}\text{Eu}$  the energy resolution was only 7.8%. The timing resolution between the  $\text{LaBr}_3(\text{Ce})$  detectors was characterized as about 330 ps (FWHM) for coincidences between the two transitions (511 and 1274.5 keV) from a  $^{22}\text{Na}$  calibration source.

The data acquisition was completed with MADC-32 (MESYTEC) and V755N (CAEN) modules associated with the VME system. The data were sorted in gated energy spectra, two-dimensional energy-energy ( $E_\gamma - E_\gamma$ ), and three-dimensional energy-energy-time ( $E_\gamma - E_\gamma - \Delta T$ ) matrices, where  $E_\gamma$  is the  $\gamma$ -ray energy detected by a  $\text{LaBr}_3(\text{Ce})$  detector and  $\Delta T$  is a time difference between two  $\gamma$  rays detected in coincidence. The time spectra were obtained with two-dimensional energy gates imposed on  $E_\gamma - E_\gamma - \Delta T$  matrices, which were gated on prompt transitions with HPGe detectors. The general data treatment of using this method can be found in detail in a publication by Mărginean *et al.* [6].

The level scheme of  $^{174}\text{Os}$  is well known [13] and most of its populated strength comes from the ground band. Figure 2(a) shows a sum spectrum of all crystals of the HPGe detectors to compare the energy resolution with an energy spectrum of the  $\text{LaBr}_3(\text{Ce})$  detectors in Fig. 2(b). At low energies, the higher efficiency of the  $\text{LaBr}_3(\text{Ce})$  with respect to the HPGe detectors is remarkable. The energies of  $\gamma$  rays in  $^{174}\text{Os}$  are marked with corresponding numbers. Finally, in Fig. 2(c) the same spectrum as in Fig. 2(b) is presented,

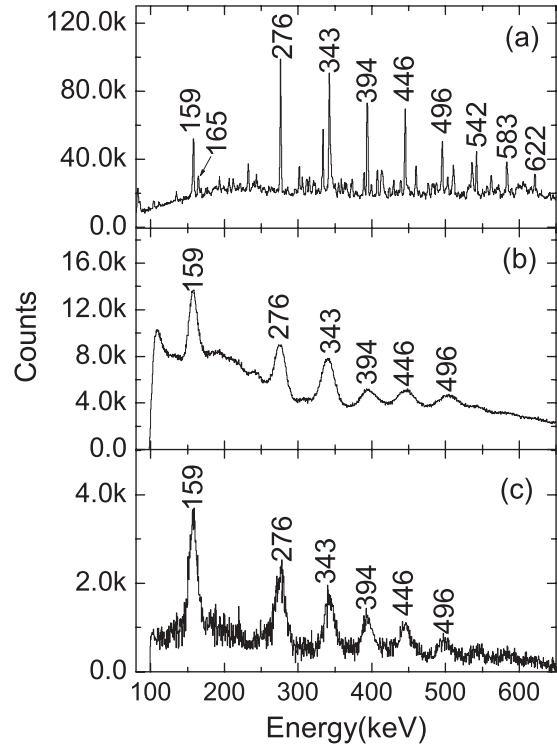


FIG. 2.  $^{174}\text{Os}$  coincidence energy spectra. (a) Total projection from all HPGe detectors. (b) Total projection from all  $\text{LaBr}_3(\text{Ce})$  detectors. (c)  $\text{LaBr}_3(\text{Ce})$  energy spectrum gated on sums of 342-, 394-, 445-, and 496-keV transitions in the HPGe detectors.

but this time in coincidence with the 343-, 394-, 446-, and 496-keV transitions from  $^{174}\text{Os}$  in the HPGe detectors, which improves the peak-to-background ratio.

Delayed coincidence time spectra for the transitions of interest were obtained by gating on the two  $\gamma$  rays on an energy-energy time difference  $\gamma\gamma\Delta T$  cube, constructed for the  $\text{LaBr}_3(\text{Ce})$  detectors gated by the HPGe detectors. Figure 3(b) shows the typical time-delayed spectrum, obtained when the start is given by the 276-keV feeding transition above the  $2_1^+$  level and the stop by the 159 keV transition deexciting the  $2_1^+$  level, respectively. With scintillators, despite the good energy resolution of  $\text{LaBr}_3(\text{Ce})$ , doublets such as the 159–165 keV one cannot be separated [see Fig. 2(c)]. However, the 165-keV transition is a contamination from  $^{175}\text{Os}$ . When the delayed time spectrum was extracted from the matrices by gating on Ge detectors, it had no contribution to the measured slope. Strictly speaking these contaminated coincidence spectra with energies near gating transitions will contain contributions due to the lifetimes of the states located at higher levels or other nuclei. However, in the present case, taking into account the intensity of these transitions, these contributions can be neglected. The background observed in the  $\gamma$ -ray singles spectra arises principally from the Compton continuum. Though gates on coincident  $\gamma$  transitions were set in the HPGe detectors, the background could not be fully eliminated, as shown in Fig. 2(c). Therefore we set a gate on the Compton spectrum just above the 159 keV peak and the events resulting from the Compton gate were subtracted from the time spectrum generated by the full-peak events. The experimental hall was

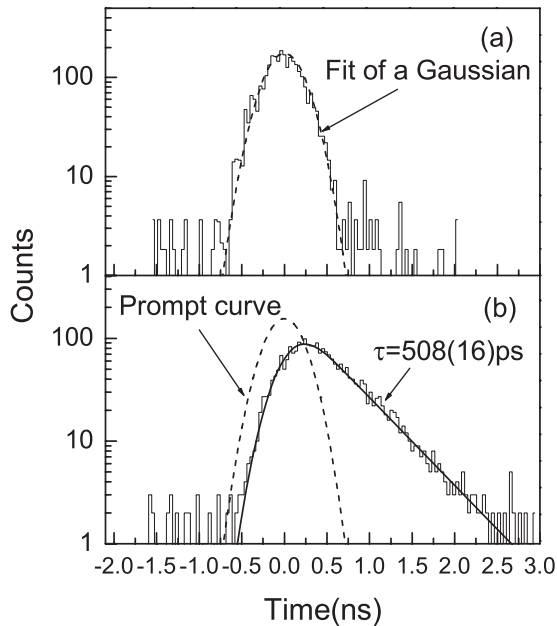


FIG. 3. Delayed coincidence time spectrum of (a) the  $4_1^+$  state and (b) the  $2_1^+$  state of  $^{174}\text{Os}$ . See text for details.

well insulated from the outside by thick concrete walls and was equipped with a forced cold air circulation which kept the temperature nearly constant. Under these conditions, a trivial drift of the centroid was observed in the time spectra and was corrected during the off-line data treatment. The delayed time spectrum of the  $4_1^+$  state is also shown in Fig. 3(a) and no exponential tail emerges in this spectrum. By this token, this level lifetime is much shorter than the detector time resolution, and known as 26.3(11) ps from the RDM measurement [9]. Therefore, in view of the timing properties of the detectors used in our experiment, the transition deexciting this level can be considered as a prompt transition and used for time calibration. The full width at half maximum (FWHM) was determined by fitting the time spectrum considered as a prompt curve using a Gaussian function in Fig. 3(a).

Finally, the time spectrum was analyzed by the shape deconvolution method [4]. As the centroid and the FWHM of the prompt time spectra slightly change as a function of  $\gamma$ -ray energy, the lifetime of the  $2_1^+$  state is determined by also fitting the position and the width of the corresponding prompt curve and finally deduced to be  $\tau = 508(16)$  ps [see the solid line in Fig. 3(b)]. Moreover, for this long lifetime even a strong variation of the FWHM value for the prompt curve has no effect on the determination of the slope and in this case the long slope provides enough data points to fit with a straight line. Therefore, alternatively, we fitted the slope part outside of the prompt region to a straight line on a logarithmic scale. This procedure gives a lifetime of  $\tau = 518(24)$  ps for the slope. Finally, the result for the lifetime of the 159-keV level is adopted as the mean of these two values:  $\tau = 513(20)$  ps, which agrees well with the value of  $\tau = 505(60)$  ps obtained using the RDM reported in the literature [9]. The modern fast timing technique used in the present experiment, however, leads to a much higher precision of the measurement.

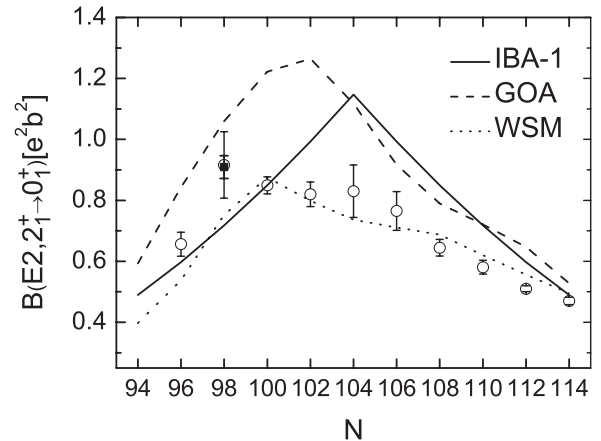


FIG. 4. Systematics of  $B(E2)$  data for the Os isotopes. The  $B(E2, 2_1^+ \rightarrow 0_1^+)$  data are taken from Ref. [10], except for  $^{176}\text{Os}$  [11],  $^{178}\text{Os}$  [12], and  $^{180}\text{Os}$  [3]. The value obtained within the present work is superimposed on the previously known experimental value with a solid square. The data are compared with the predictions of several models. See text for details.

In Fig. 4, the experimentally known  $B(E2, 2_1^+ \rightarrow 0_1^+)$  values for Os isotopes including the present data are plotted as a function of the neutron number. The  $B(E2, 2_1^+ \rightarrow 0_1^+)$  transition strengths of these nuclei should directly correlate to the size of the valence space and maximize at the midshell. However, the experimental  $B(E2, 2_1^+ \rightarrow 0_1^+)$  values seem to have a maximum at  $N = 98$ , although the experimental uncertainty of the  $B(E2, 2_1^+ \rightarrow 0_1^+)$  value of  $^{180}\text{Os}$  is not small enough. The result suggests that the deformation of the nuclear shape will be enhanced at  $N = 98$ . For comparison, transition rates were calculated using the interacting boson approximation model (IBA-1) [14]. Clearly, the simple valence nucleon version of the IBA-1 model gives an overly strong particle number dependence, and thus fails to reproduce the overall behavior of these  $B(E2, 2_1^+ \rightarrow 0_1^+)$  values, especially by expecting a maximal value at the neutron midshell  $N = 104$ . As mentioned above, our new value for  $^{174}\text{Os}$  is still the maximum value lying even slightly higher than the value found in  $^{180}\text{Os}$  at the neutron midshell. The fact that the result for  $^{174}\text{Os}$  presented here, obtained in a fast timing measurement, is in accordance with the previously published value obtained via the RDM [9], renders it unlikely that the high  $B(E2, 2_1^+ \rightarrow 0_1^+)$  value of this nucleus is due to an error in measurement, as was suggested by the authors of Ref. [3].

In fact, many theoretical calculations in the literature have been devoted to the even-even Os isotopes and especially to the description of the related  $B(E2, 2_1^+ \rightarrow 0_1^+)$  transition strengths [3]. In Fig. 4, we also show calculations with a Gogny force [15] for  $B(E2, 2_1^+ \rightarrow 0_1^+)$  of Os isotopes compared with the experimental data. This model describes qualitatively the data, and the discrepancy with respect to the reproduction of the absolute values might be compensated for by a scaling factor. However, this model predicts a peak of the  $B(E2, 2_1^+ \rightarrow 0_1^+)$  value at  $N = 102$ . The systematics of the experimental  $B(E2, 2_1^+ \rightarrow 0_1^+)$  values, with the significantly high value for  $^{174}\text{Os}$  from this experiment, clearly indicates that a maximum in the  $B(E2, 2_1^+ \rightarrow 0_1^+)$  dependence on  $N$ , or at

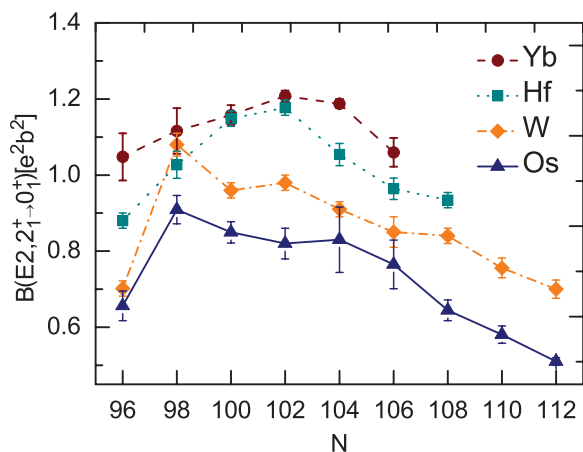


FIG. 5. (Color online) Evolution of experimental  $B(E2, 2_1^+ \rightarrow 0_1^+)$  values of even-even Yb, Hf, W, and Os isotopes. Data from Nuclear Data Sheets. Exceptions are as follows:  $^{176}\text{Os}$  [11],  $^{178}\text{Os}$  [12],  $^{180}\text{Os}$  [3],  $^{172,178}\text{W}$  [2],  $^{174}\text{W}$  [16],  $^{176}\text{W}$  [17],  $^{168}\text{Hf}$  [17], and  $^{172,174}\text{Hf}$  [18]. Lines connecting experimental values are drawn to guide the eye.

least a sharp rise in their values, should be at  $N = 98$ . None of these models reproduces this dependence. Another calculation made with the Woods-Saxon model in the compilation of Raman *et al.* [10] is also presented in Fig. 4. This calculation predicts a maximum in the  $B(E2, 2_1^+ \rightarrow 0_1^+)$  dependence at  $N = 100$ . In fact, the predictions of this model give the best agreement with the overall experimental results, except for a large deviation at  $^{174}\text{Os}$ . An interesting outcome of this work is that in the Os isotopes, there seems to be a maximum in the  $B(E2, 2_1^+ \rightarrow 0_1^+)$  dependence on  $N$ , not at the midshell, as expected, but at a lower value of  $N$ . Apparently, further efforts are expected to reproduce the detailed overall description of the data, especially detailed microscopic calculations.

To understand the development of collectivity in the even-even Os chain and to help determine its nature, it is interesting to consider the Os data within regional systematics. The reduced transition probabilities of the first  $2^+$  states versus neutron number for  $70 \leq Z \leq 76$  even-even nuclei are shown in Fig. 5. From the figure, one observes that the evolution of  $B(E2, 2_1^+ \rightarrow 0_1^+)$  values in the neighboring even-even W isotopes seems to have the same shape as that of the Os isotopes and a clear bump at  $N = 98$ , while there is a maximum for Yb and Hf near or at the neutron midshell. We speculate that the anomalous behavior at  $N = 98$  could be attributed to a local

shell structure at  $N = 98$  in the Nilsson neutron orbitals [19]. The presence of the anomalies of  $B(E2, 2_1^+ \rightarrow 0_1^+)$  in  $^{172}\text{W}$  and  $^{174}\text{Os}$  may be a jump in deformation because of this neutron subshell effect, while it seems not to be large enough to change the  $^{168}\text{Yb}$  and  $^{170}\text{Hf}$  to a much more deformed shape. This brings about the natural question of whether it is possible that the anomalous behavior of  $^{172}\text{W}$  and  $^{174}\text{Os}$  originate also from the contributions of protons. This can be understood intuitively since, in the nuclei with  $Z = 74$  and  $76$ , the Fermi levels are close to the  $\frac{1}{2}[541]$  component of the  $h_{9/2}$  orbital [9]. Nuclei in the well-deformed rare-earth region are known to possess stable nuclear shapes with a prolate deformation. However, at the edge of the deformed region the nuclear potential becomes soft and, consequently, may result in shape coexistence [20]. Therefore, low  $\Omega_{\frac{1}{2}}[541]$  orbitals from the  $h_{9/2}$  parentage for W and Os isotopes favor a large deformation. That is, the present anomalously high transition strengths for the  $2_1^+$  states in  $^{172}\text{W}$  and  $^{174}\text{Os}$  could possibly be explained as arising from both the effects of the deformed subshell at  $N = 98$  and the proton  $h_{9/2}$  orbital. Recently, Rudigier *et al.* [2] proposed that a large hexadecapole  $\beta_4$  effect could play a role in these particular nuclei. Although the heavier W and Os isotopes have large negative  $\beta_4$  values [21,22], it is still beyond our imagination that the lighter nuclei of  $^{172}\text{W}$  and  $^{174}\text{Os}$  have a  $\beta_4$  value larger than 0.1. Thus, experimental  $\beta_4$  values are needed to test their idea. It would be interesting to know if the platinum isotopes around  $N = 98$  follow a trend similar to that of the tungsten and osmium isotopes. Unfortunately, in most of the corresponding Pt isotopes the  $B(E2, 2_1^+ \rightarrow 0_1^+)$  values are unknown or have large uncertainties.

In summary, the lifetime of the  $2_1^+$  state in  $^{174}\text{Os}$  has been remeasured in a fast timing experiment and determined with better precision to be  $\tau = 513(20)$  ps. The small error makes this value sufficiently precise to serve as a normalization parameter for meaningful tests of relevant models. The systematics of  $B(E2, 2_1^+ \rightarrow 0_1^+)$  indicate that the deformation reaches a maximum at  $N = 98$  for W and Os isotopes, which can be attributed to both the effect of the deformed subshell at  $N = 98$  and the proton “intruder”  $h_{9/2}$  orbital.

We would like to thank the HI-13 tandem accelerator staff for the smooth operation of the machine. We are grateful to Dr. Q. W. Fan and Professor G. J. Xu for their assistance during target preparation. This work is partially supported by the National Natural Science Foundation of China under Contracts No. 10927507, No. 11075214, No. 10675171, and No. 11175259.

- [1] F. Iachello, *Phys. Rev. Lett.* **87**, 052502 (2001).
- [2] M. Rudigier *et al.*, *Nucl. Phys. A* **847**, 89 (2010).
- [3] O. Möller *et al.*, *Phys. Rev. C* **72**, 034306 (2005).
- [4] H. Mach, R. L. Gill, and M. Moszyński, *Nucl. Instrum. Methods A* **280**, 49 (1989).
- [5] E. R. White *et al.*, *Phys. Rev. C* **76**, 057303 (2007).
- [6] N. Mărginean *et al.*, *Eur. Phys. J. A* **46**, 329 (2010).
- [7] S. Zhu *et al.*, *Nucl. Instrum. Methods A* **652**, 231 (2011).
- [8] S. Kisyov *et al.*, *Phys. Rev. C* **84**, 014324 (2011).

- [9] J. Gascon *et al.*, *Nucl. Phys. A* **470**, 230 (1987).
- [10] S. Raman, C. W. Nestor Jr., and P. Tikkanen, *At. Data Nucl. Data Tables* **78**, 1 (2001).
- [11] B. Melon, Ph.D. thesis, Universität zu Köln (in Germany), 2011.
- [12] A. Dewald *et al.*, *J. Phys. G: Nucl. Part. Phys.* **31**, S1427 (2005).
- [13] E. Browne and J. D. Huo, *Nucl. Data Sheets* **87**, 15 (1999).

- [14] E. A. McCutchan and N. V. Zamfir, *Phys. Rev. C* **71**, 054306 (2005).
- [15] G. F. Bertsch *et al.*, *Phys. Rev. Lett.* **99**, 032502 (2007).
- [16] V. Werner *et al.*, *J. Phys.: Conf. Ser.* **312**, 092062 (2011).
- [17] J. M. Régis *et al.*, *Nucl. Instrum. Methods Phys. Res., Sect. A* **606**, 466 (2009).
- [18] J. M. Régis, Ph.D. thesis, Universität zu Köln (in Germany), 2011.
- [19] F. S. Stephens, N. Lark, and R. M. Diamond, *Rev. Lett.* **12**, 225 (1964).
- [20] B. Cederwall *et al.*, *Nucl. Phys. A* **545**, 871 (1992).
- [21] F. T. Baker *et al.*, *Nucl. Phys. A* **258**, 43 (1976).
- [22] I. Y. Lee *et al.*, *Phys. Rev. C* **12**, 1483 (1975).